PAPER

Microencapsulation of *Citrus aurantifolia* essential oil with the optimized CaCl$_2$ crosslinker and its antibacterial study for cosmetic textiles†

Luthfia Pratiwi, [ID] [a] Diana Rakhmawaty Eddy, [ID] [a] Jamaludin Al Anshori, [ID] [a] Asep Harja, [b] Tatang Wahyudi, [c] Agus Surya Mulyawan [c] and Euis Julaeha [ID] *[a]

A functional fabric immobilized by the microcapsules of *C. aurantifolia* lime essential oil (LO) was prepared and characterized. A varied amount of CaCl$_2$ crosslinker was optimized to coacervate LO using alginate–gelatin biopolymers and Tween 80 emulsifier. A further evaluation of the immobilized LO microcapsules for the antibacterial effect against both Gram-positive and Gram-negative bacteria was conducted. The optimized alginate/gelatin-based microcapsules were effectively crosslinked by 15% CaCl$_2$ with an yield, oil content (OC), and encapsulation efficiency (EE) of 39.91 ± 3.10%, 78.33 ± 7.53%, and 90.27 ± 5.84%, respectively. A spherical shape of LO microcapsules was homogeneously found with an average particle size of 1.394 μm. A first-order kinetics mechanism for the release of LO out of the microcapsules was modeled by Avrami's kinetic equation ($k = 1.60 ± 3.68 \times 10^{-5}$ s^{-1}). The LO microcapsules demonstrated good thermal stability up to 100 °C and maintained 51.07% OC and 43.56% EE at ambient temperature for three weeks. Using a pad dry method and citric acid binder, LO microcapsules were successfully immobilized on a cloth with a % add on 30.60 ± 1.80%. The LO microcapsules and the immobilized one exhibited a moderate ZoI of bacterial growth for Gram-positive *S. aureus* and *S. epidermidis* as well as Gram-negative *E. coli* and *K. pneumonia*. Further washing test toward the functional fabric showed that the LO microcapsules incorporated into the fabric were resistant to five cycles of normal washing with a mass reduction of 22.01 ± 1.69%.

Introduction

The essential oil of *C. aurantifolia* (LO), obtained from its peels, has been reported to exhibit antimicrobial activities, which is due to the chemical compositions of limonene, citral, caryophyllene, linalool, and terpinene.[1] It is known that δ-limonene was found as the main chemical component of LO, which contributed to the strong scent and antibacterial potency against typical Gram-positive (*Bacillus subtilis*, *Enterococcus durans*, *Enterococcus hirae*, *Listeria monocytogenes*, *Staphylococcus aureus*, and *Staphylococcus epidermidis*) and Gram-negative (*Enterobacter cloacae*, *Escherichia coli*, *Pseudomonas aeruginosa*, *Serratia marcescens*, and *Salmonella typhi*) bacteria.[2–4] In addition, LO was also found to be active against

[a]Department of Chemistry, Faculty of Mathematics and Natural Sciences, Universitas Padjadjaran, Jl. Raya Bandung-Sumedang km.21, Jatinangor, Sumedang, 45363, West Java, Indonesia. E-mail: euis.julaeha@unpad.ac.id

[b]Department of Geophysics, Faculty of Mathematics and Natural Sciences, Universitas Padjadjaran, Jl. Raya Bandung-Sumedang km.21, Jatinangor, Sumedang, 45363, West Java, Indonesia

[c]Center for Textile, Jl. Jendral Ahmad Yani No.390, Bandung, 40272, West Java, Indonesia

† Electronic supplementary information (ESI) available. See DOI: https://doi.org/10.1039/d2ra04053k

Streptococcus bacteria, namely *S. salivarius*, *S. mutans*, *S. sobrinus*, *S. mitis* and *S. sanguinis* and *Lactobacillus casei*.[5] Recently, the peels of LO exhibited an excellent *in vitro* antibacterial activity against the isolates of multidrug-resistant bacteria (*E. coli* (B1), *Klebsiella* sp., *S. aureus*, *K. pneumonia*, *P. aeruginosa*, *Shigella* sp., *S. aureus*, MRSA (N18), MRSA (N11), *Streptococcus pneumoniae*, and *E. coli* (EK58)).[6]

A redesigned packaging approach is necessary to increase the use of the essential oil of *C. aurantifolia* (LO) in daily life applications, which is hindered by their features such as volatility, readily decomposed by oxygen, air, temperature radiation, light, humidity, pH conditions, and water.[7–13] Among the available preservation methods for such environmentally sensitive agents, microencapsulation with a simple and easy complex coacervation becomes an interesting method to be explored. Employing biopolymers of alginate–gelatin crosslinked by glutaraldehyde, microencapsulation was successfully performed to coacervate a drug core of metronidazole hydrochloride, diclofenac sodium, and indomethacin,[14] an ascorbic acid,[15] lemongrass essential oil,[16] and *C. aurantifolia* essential oil.[17–19] On the other side, the same biopolymers crosslinked by CaCl$_2$ coacervated a procyanidin,[20] and *Black pepper* essential oil efficiently.[21] The crosslinker is an essential component in the coacervation process, which serves to harden the shells and

stabilize the microcapsule structure.[12] In particular, the shell rigidity, storage stability of microcapsules, and their thermomechanical properties are improved.[12] Although aldehyde-based crosslinkers such as glutaraldehyde are generally recognized as efficient binders, their toxicity still remains a problem upon excessive utilization, especially for cosmetic textiles.[22–25] On the other hand, the non-toxic $CaCl_2$ crosslinker can bind a biopolymer like sodium alginate, forming a stable three-dimensional network of "egg-box". Upon a crosslinking process of the shells with the linker, an ionic interaction occurred between the calcium ion and the carboxyl group of the residue block of the guluronic acid (G) of the two adjacent alginate chains.[26,27]

Currently, textiles are not only designed for aesthetic purposes but are also expected to have an extra functional value such as a cosmetic function.[28] Cosmetic textiles are textiles containing long-lasting cosmetic ingredients that are released from time to time on parts of the human body, especially the skin, which have special functions like UV protection, body slimming, vitalizing, moisturizing, fragrance, refreshing, relaxing, skin elasticity, and antibacterial activity.[29] Several textiles containing antibacterial agents such as TiO_2,[30,31] ZnO, quaternary ammonium salt, polybiguanide, N-halamine,[31] and silver nanoparticles[32] are already available on the market. Indeed, most of them are synthetic, expensive, and not environmentally friendly.[25,30] On the other hand, alternative agents which exhibit safer and healthier properties are getting more attention from consumers. Among the green antibacterial agents are essential oils, which are based on natural products.

To the best of our knowledge, microencapsulation of antibacterial LO using an alginate–gelatin shell and $CaCl_2$ crosslinker for cosmetic textiles has not been reported. Therefore, herein, coacervation of LO by alginate–gelatin biopolymers which was crosslinked by the optimized amount of $CaCl_2$ was reported. In addition, the characterization and the antibacterial activities of the LO microcapsules and the cotton immobilized microcapsules were also included.

Results and discussion

LO microencapsulation and characterization

The LO was obtained by using hydrodistillation with a 0.38% yield. The amount of the isolated LO was still marginally consistent with the yield obtained elsewhere (0.2–2%).[19,33–37] Such a result is reasonable because geographical conditions, climate, season, and maturity of the fruits considerably influence the LO yield.[38,39] The resulting LO exhibited a distinctive lime scent with a pale-yellow color. The four main components of the LO, δ-limonene (22.22%), citral (18.23%), β-pinene (14.60%), and 2,6-dimethyl-1,3,5,7-octatetraene,E,E-(14.21%), remained as the major compounds (ESI Table 1†).

Upon coacervation of the LO by alginate–gelatin shells at various amounts of $CaCl_2$ crosslinker, the yield of the microcapsules varied from 35 to 41%, yet statistically was not different (Table 1). The optimum amount of the microcapsules was obtained at 10–20% crosslinker. The related microcapsules showed encapsulation efficiency (EE) and oil content (OC)

Table 1 The yield of LO microcapsules crosslinked by various amounts of $CaCl_2^a$

Amount of $CaCl_2$ crosslinker/%	Yield[b]/%
10	40.12 ± 1.68^{bc}
15	39.91 ± 3.10^{abc}
20	41.64 ± 1.24^{c}
25	35.87 ± 2.01^{a}
30	36.96 ± 2.14^{ab}

[a] [a–c] There was no significant difference between the groups as shown by the mean value followed by the same letter. [b] $n = 3$; data reported as mean $\pm$ SD. A 95% confidence level statistical test of significant difference was performed. One way ANOVA results showed a significant difference between all treatments at $P = 0.039$.

ranging from 69–93% and 66–78% respectively (Table 2). In general, the highest % OC value was gained up to 78% by 15% of crosslinkers, yet statistically didn't show a subtle difference between all the treatments. However, the statistical analysis of % EE at various amounts of the crosslinkers was substantially different, where the highest efficiency of 93% was procured by 20% of crosslinkers. The higher the % EE value, the more efficient the microencapsulation process takes place. Thus better stability and longer shelf life will be attained.[12,40] Finally, the 15% crosslinker was successfully enhancing % OC and % EE inside the alginate/gelatin shells compared to the $CaCl_2$[21] and glutaraldehyde.[18]

Microcapsule characterization

To determine the particle size of the microcapsules and their distribution, characterization with a particle size analyzer (PSA) was performed.[41] The PSA results showed that the size of the microcapsules obtained at the various amounts of crosslinker was in the range of 1.364–1.564 μm (Fig. 1 and ESI Fig. 1†). Based on their ratio of mean/median (0.937–0.984 μm) which was close to one, all the microcapsules formed a well-
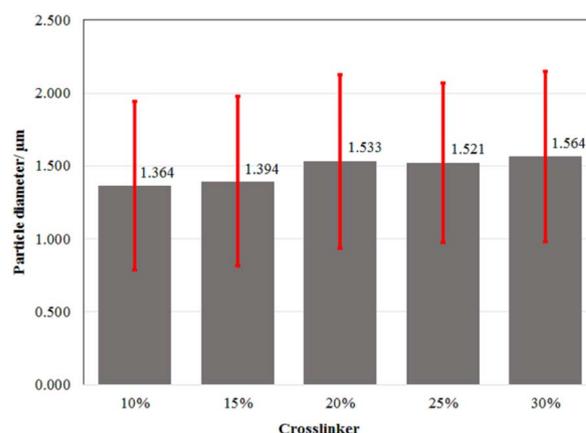

Fig. 1 Average particle size distribution of LO microcapsule crosslinked at the various amounts of $CaCl_2$. A 95% confidence level statistical test of significant difference was performed. One-way ANOVA's P-value of 1.000 indicates that there is no significant difference between any of the treatments.
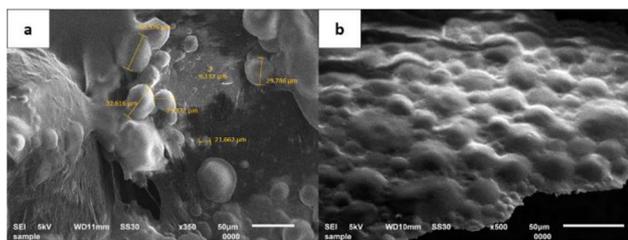
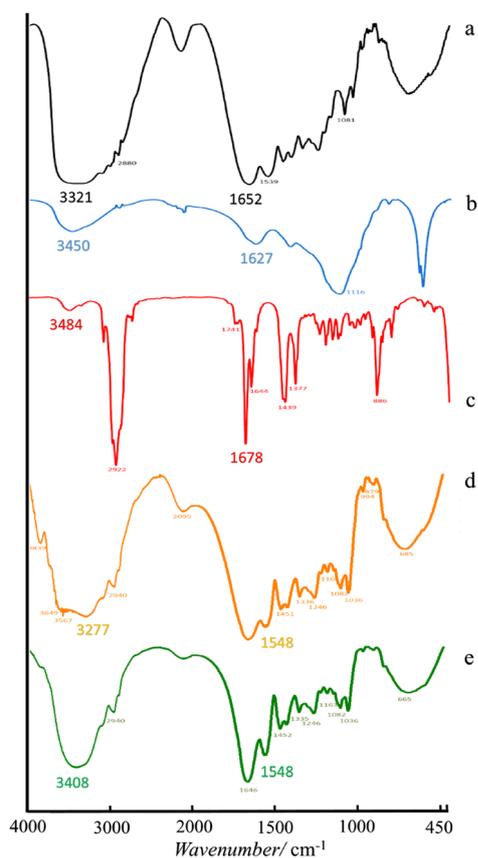Fig. 2 SEM micrograph of LO microcapsules crosslinked by 15% $CaCl_2$: magnifications of (a) 350× and (b) 500×.

Fig. 3 Spectra of FTIR of (a) gelatin, (b) sodium alginate, (c) LO, (d) coreless microcapsules, and (e) LO microcapsules.

the LO core (Fig. 3). The FTIR spectrum of gelatin is shown in Fig. 3a. The signal at 3321 cm^{-1} revealed the NH_2 moiety of gelatin. In addition, functional groups of amides C=O and amine C–N were also assigned at 1652 cm^{-1} and 1081 cm^{-1} respectively. On the other hand, the FTIR spectrum of sodium alginate (Fig. 3b) indicated groups of –OH at 3450 cm^{-1}, a carboxylate C=O at 1627 cm^{-1} and C–O of an ester at 1116 cm^{-1}. Although the LO consisted of several compounds, its FTIR spectrum (Fig. 3c) could still distinguish representative major moieties of the mixture. Such characteristic peaks at 3484 cm^{-1} (–OH); 2922 cm^{-1} (aliphatic C–H); 1741 cm^{-1} and 1678 cm^{-1} (C=O); and 1644 cm^{-1} (C=C) were sharply observed. Upon the encapsulation process, the amine and carboxylate groups of gelatin were observed at 3321 and 1652 cm^{-1} respectively (Fig. 3a), and the alginate hydroxyl group at 3450 cm^{-1} (Fig. 3b) remained distinct (Fig. 3d and e). Such a non-covalent interaction between all those moieties presumably developed. A similar finding was also reported previously for alginate/gelatin microcapsules crosslinked by $CaCl_2$,[21] glutaraldehyde[18] and genipin.[15] The non-covalent interaction between two ionic biopolymers like gelatin and sodium alginate tends to be more prominent under an acidic condition.[14] Correspondingly, an original LO signal (Fig. 3c) barely overlapped with other signals of the LO microcapsules (Fig. 3e), which was further confirmed with the coreless microcapsules (Fig. 3d).
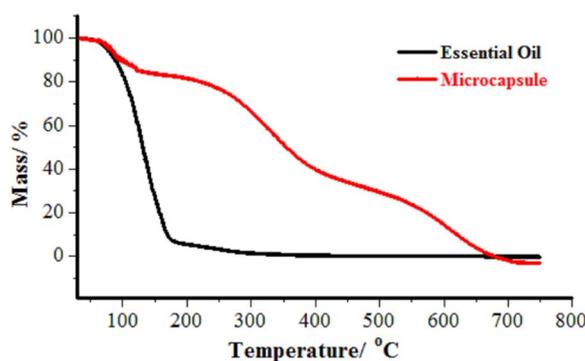

Fig. 4 TGA thermograph of (—) LO and (—) LO microcapsules.

distributed particle size and homogeneity. Additional statistical analysis revealed that there were no significant differences in the average size of all the microcapsules across all treatments. According to the Scanning Electron Microscope (SEM) micrograph of the LO microcapsules crosslinked by 15% $CaCl_2$ (Fig. 2), spherical and agglomerated microcapsules were mostly observed. Presumably, the type of $CaCl_2$ crosslinker resulted in a better rigidity of the microcapsule structure[23] than glutaraldehyde,[14,18] and perhaps favors better retention release of the core material.[42]

Further Fourier Transform Infrared (FTIR) spectroscopy analysis of the microcapsules discovered the moieties and confirmed typical interactions between the shell materials and

Table 2 Oil Content (OC) and Encapsulation Efficiency (EE) of LO microcapsules crosslinked by various amounts of $CaCl_2{}^a$

Amount of $CaCl_2$ crosslinker/%	OC^b/%	EE^b/%
10	70.38 ± 6.13[a]	81.61 ± 4.45[ab]
15	78.33 ± 7.53[a]	90.27 ± 5.84[b]
20	77.39 ± 6.92[a]	93.21 ± 7.57[b]
25	66.71 ± 15.33[a]	69.14 ± 15.60[a]
30	70.84 ± 3.85[a]	75.94 ± 7.67[ab]

^{a} [a–c] There was no significant difference between the groups as shown by the mean value followed by the same letter. ^{b} $n = 3$; data reported as mean ± SD. A 95% confidence level statistical test of significant difference was performed. There was no significant difference in OC, as demonstrated by the one way ANOVA value of $P = 0.057$. There was a significant difference in EE, as demonstrated by the one-way ANOVA value of $P = 0.046$.

© 2022 The Author(s). Published by the Royal Society of Chemistry

Thereby, no substantial covalent interaction was discovered between the LO core and its shells. It was implied that the physical interaction of the LO core with the shells must have existed, so the LO core could still be released through the micropores easily.

Further thermal stability was then tested with the microcapsules crosslinked with 15% crosslinker at 0–750 °C as the representative. The thermograph (Fig. 4) showed that only 10.3% of the mass of the LO microcapsules was lost during the initial heating stage (100 °C). At this temperature, water moisture and a portion of LO may have evaporated. Rapid mass loss of 60% of LO microcapsules was then observed upon heating at the second stage (100–400 °C). At this stage, most of the LO core should be evaporated instead of initial shell degradation. Finally, more than 60% of the mass was remarkably lost at the last stage of heating (>400 °C), which was plausibly caused by depolymerization and decomposition.[43] As anticipated, the uncoated LO (black line) just diminished at 100 °C to 170 °C.

LO release of microcapsules and their kinetics. The protection performance of the various LO microcapsules towards mechanical and chemical intervention has been further studied. The encapsulated LO was released gradually upon sonication and chemical extraction in 2 h (Fig. 5). Among all the microcapsules, the 15% crosslinkers was the optimum concentration to strengthen the shells firmly, thus holding the LO core up to 73%. Based on the Avrami equation,[44–47] the
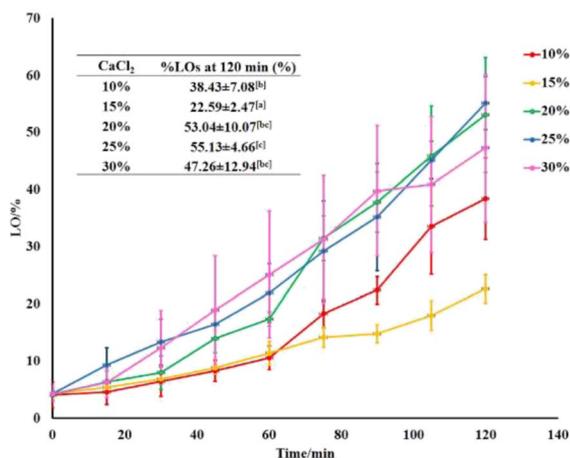

Fig. 5 LO release performance out of microcapsules at various amounts of crosslinkers.
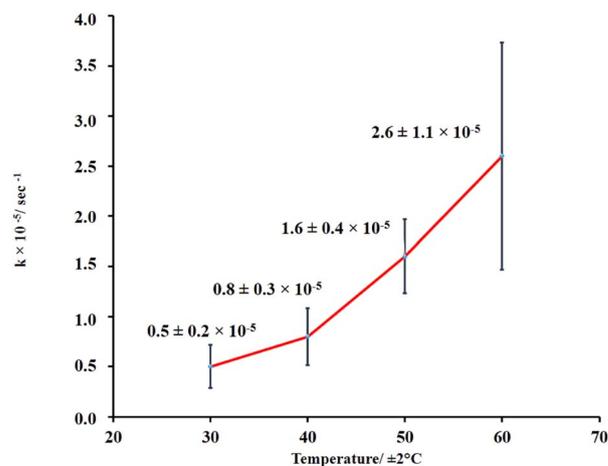

Fig. 6 LO release performance out of microcapsules at various temperatures.

release rate constant of the microcapsules with 15% crosslinkers was the lowest one out of the others (Table 3). According to the computed n value of Avrami's equation, the LO release mechanism was ruled by the first-order kinetics for all microcapsules. In addition, the R^2 values calculated from the linear regression assured that the LO released from all the microcapsules were best fitted to Avrami's kinetic model (ESI Fig. 2–6†). Comparatively, the 15% $CaCl_2$ crosslinker successfully enhanced the retention of the LO inside the alginate/gelatin shells by one order of magnitude of rate constant compared to the glutaraldehyde one[18] and genipin,[15] even compared to the chitosan/gum arabic shell.[48] Thereby, the microcapsule shells of alginate/gelatin crosslinked by $CaCl_2$ were confirmed indirectly to have better density than those crosslinked by glutaraldehyde; thus, the LO overlaid stronger inside the capsules. The LO might be kept even longer inside the microcapsules under normal conditions, where no chemical or excessive mechanical interferences are used.

Further investigation of LO microcapsule release at various temperatures was also performed (Fig. 6, and ESI Fig. 7–10†). The range of the applied temperature (30–60 °C) represented the ambient temperature and the normal washing condition of textile materials. Overall, the release rate constant of the LO microcapsules was linearly increasing with the elevated temperature. However, under the applied max temperature of 60 °C, the release rate was still preserved at the order of 10^{-5} s^{-1} and even slower by one order of magnitude compared to the similar LO microcapsules crosslinked by glutaraldehyde.[18]

Table 3 The Avrami's kinetic data of LO release out of the microcapsules at the various amounts of crosslinker[a]

Amount of $CaCl_2$ crosslinker/%	$k \pm SD/s^{-1}$	$n \pm SD$	R^2
10	$5.79 \pm 2.84 \times 10^{-5}$	1.19 ± 0.41	0.9034
15	$1.60 \pm 3.68 \times 10^{-5}$	0.72 ± 0.07	0.9363
20	$6.57 \pm 4.12 \times 10^{-5}$	1.14 ± 0.28	0.9208
25	$8.50 \pm 1.39 \times 10^{-5}$	1.01 ± 0.09	0.9141
30	$9.33 \pm 4.05 \times 10^{-5}$	1.14 ± 0.28	0.9937

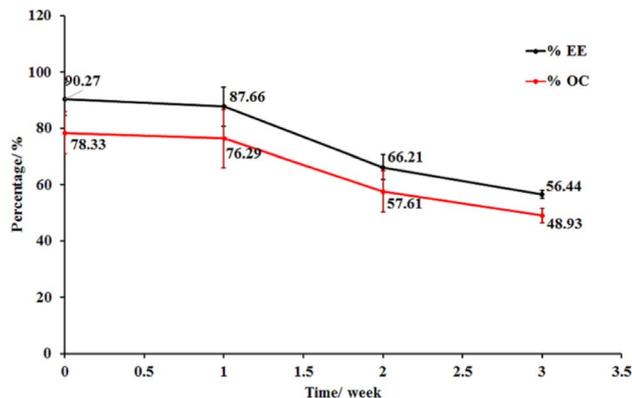[a] Data were expressed as mean $\pm$ SD; $n = 3$.

Fig. 7 Stability of LO microcapsules at room temperature (mean ± SD, $n = 3$).

Microcapsule storage stability. The storage stability of the LO microcapsules crosslinked with 15% $CaCl_2$ was evaluated under ambient conditions (Fig. 7). The reduction of 49% of OC and 56% of EE was observed in the capsules in three weeks. The coating's physical and chemical alterations as well as the oil diffusion were linked to the capsule's disintegration. This is in line with Timilsena *et al.* (2020), who discovered the high dependency of microcapsule stability on the structure and functionality of the coating matrix, processing conditions, and the interaction of the coating with the core, if any.[12] However, with increasing storage time, the amount of oxygen absorbed into the interior of the

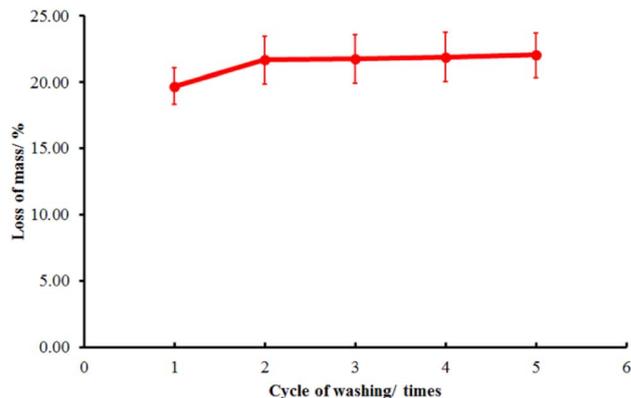**Fig. 8** Reaction between alginate, citric acid, and cotton cloth.[50]

Fig. 10 Washing test of the immobilized LO microcapsules (mean ± SD, $n = 2$).

microcapsule increased, resulting in the formation of peroxides inside the capsule.[49]

Immobilization of microcapsules

The immobilization of the LO microcapsules was carried out using the pad dry method on cotton cloth using a sodium phosphate catalyst and a citric acid binder. An increase of the % add on up to 30.60 ± 1.80% was experienced by the immobilized fabric. The mass addition of the fabric was plausibly caused by the interaction between the LO microcapsules and the fabric over an ester bond between the hydroxyl group (–OH) of the cotton cloth and alginate with the carboxylic moieties (–COOH) of citric acid[50] (Fig. 8).

The attachment of the LO microcapsules onto the fabric was further confirmed by the SEM micrograph (Fig. 9). The morphology of the fabric before (Fig. 9a) and after being embedded by the LO microcapsules (Fig. 9b and c) was distinctively revealed. Undeniably, most of the incorporated LO microcapsules were still agglomerated.

The washing strength of the immobilized LO microcapsules was then tested using a Launder O-meter to ascertain their durability (Fig. 10). Upon the first cycle of washing, the mass decrease was 19.72 ± 1.38%. However, the following cycle of washing resulted in only a subtle decrease in the fabric mass
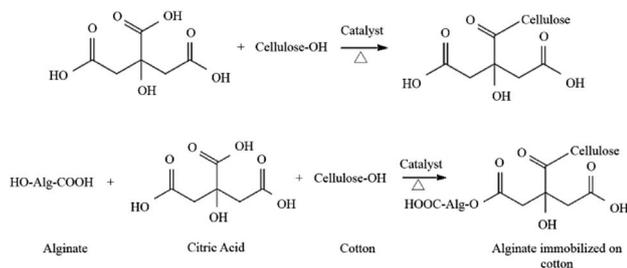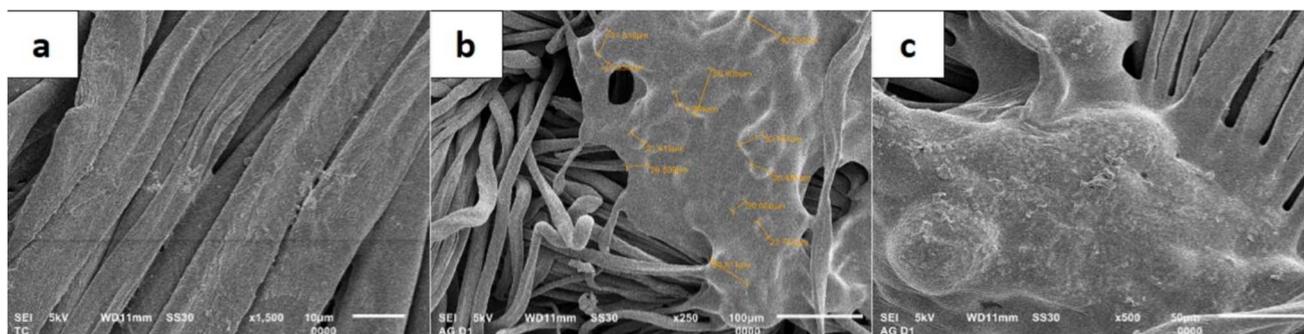

Fig. 9 SEM micrograph of (a) a fabric without microcapsules; (b) a fabric containing microcapsules at 250× magnification; (c) a fabric containing microcapsules at 500× magnification.

Table 4 The zone of inhibition (ZoI) of bacterial growth of LO, LO microcapsules, limonene, a fabric containing microcapsules, and control

| Samples | Zone of inhibition (ZoI/mm)^a | | | |
| | Gram-positive typical bacteria | | Gram-negative typical bacteria | |
	S. aureus	S. epidermidis	E. coli	K. pneumonia
LO	18.33 ± 0.46^b	33.83 ± 1.03^c	11.28 ± 0.04^c	31.95 ± 0.64^e
Limonene	7.15 ± 0.07^a	8.40 ± 0.57^a	8.40 ± 0.14^a	22.65 ± 0.64^d
Microcapsules	7.13 ± 0.04^a	8.20 ± 0.14^a	9.80 ± 1.13^b	9.10 ± 0.14^a
Test cloth	7.55 ± 0.21^a	7.50 ± 0.14^a	8.15 ± 1.56^a	15.10 ± 0.49^c
Control cloth	N.a	N.a	N.a	N.a
Amoxicillin positive control (100 ppm)	31.33 ± 0.18^c	12.05 ± 0.78^b	$10.68 \pm 0.04^{b,c}$	10.35 ± 0.14^b
Negative control n-hexane	N.a	N.a	N.a	N.a

^{a} N.a. = not active, $n = 3$; data reported as mean $\pm$ SD. A 95% confidence level statistical test of significant difference was performed. One way ANOVA results showed a significant difference between all treatments at $P = 0.000$. There was no significant difference between the groups as shown by the mean value followed by the same letter [a–e].

$(22.04 \pm 1.69\%)$. The first cycle of washing should cause the larger microcapsule particles to separate certainly from the fabric, yet the smaller ones tend to resist.[51]

Antibacterial activity

The Kirby Bauer method was used to measure the antibacterial potency of the LO microcapsules immobilized on the textiles (Table 4). Overall, the microcapsule's antibacterial assay before and after being attached to the fabrics exhibited a moderately sensitive Zone of Inhibition (ZoI).[52] Nonetheless, the antibacterial effectiveness of the modified fabrics was at least 2–4 times lower than that of the LO themselves. A slow-diffusion kinetics profile of the LO to the surface of the shells might be the reason; thus, less concentration was available. Certainly, the antibacterial synergistic effect of the LO components still remained, in a way of altering the cell membrane permeability. Therefore, the bacteria cell loss of intracellular constituents is necessary for maintaining the viability of bacteria.[53]

Experimental

Ingredients

Lime peel samples (C. aurantifolia) were obtained from the Caringin Main Market, Bandung, Indonesia, while the cotton fabrics with particular specifications (Table 5) were obtained from the Bandung Textile Center. Pro-analyst chemicals such as acetone, anhydrous sodium sulfate, citric acid, glacial acetic acid, CaCl$_2$, n-hexane, and sodium dihydrogen phosphate dihydrate were purchased from Merck. In addition, several technical-grade

Table 5 Specifications of cotton fabric

Parameter	Relevant value
Heavy	119 g m^{-2}
Tetal warp thread	84 strands per inch
Weft thread thickness	66 strands per inch
No. warp and weft yarn	Ne$_1$ 321
Composition	100% cotton
Webbing	Plain 1/1

chemicals such as gelatin, sodium alginate, and Tween-80 were obtained from PT. Subur Jaya Kimia in Bandung, Indonesia.

Preparation of LO

The preparation of LO adhered to the methodology used by Ferhat et al. (2016).[54] Lime peel (C. aurantifolia), which had been removed from the fruit, was rinsed with water before being hydrodistilled at 100 °C for three hours. The collected LO was then refrigerated after being dried over anhydrous sodium sulfate. GC-MS analysis was accomplished to determine the LO's chemical composition.

LO microencapsulation

The microencapsulation method was according to Julaeha et al. (2021). Upon 60 ± 1 °C, 0.8 g of Tween 80 and 2 g of LO were added to a solution of 3 g of gelatin in 140 mL of aqua-distilled while it was being agitated at 600 rpm. The sodium alginate solution (0.8 g in 40 mL of aqua-distilled) was then added and agitated for a further 15 minutes. The mixture was then treated with 2.5% (v/v) glacial acetic acid to raise the pH to 3.75 before being chilled to 10 °C. Once the microcapsules developed in the solution, 475 µL of 10% CaCl$_2$ crosslinker was added slowly (10%, 15%, 20%, 25%, and 30%). To finish the crosslinking reaction, the solution's temperature was eventually increased to 35 °C and agitated for an additional 3 hours. The stirred microcapsule suspension was then cooled at ambient temperature and filtered. The obtained microcapsules were then washed subsequently with water and n-hexane, to remove the remaining unreacted materials.

The yield of the LO microcapsules obtained was calculated by eqn (1).

$$\text{Yield (\%)} = \frac{\text{W2 (g)}}{\text{W1 (g)}} \times 100\% \tag{1}$$

where W1 = initial mass used (g) and W2 = mass obtained (g).

Characterization of LO microcapsules

Measurement of oil content and encapsulation efficiency. Based on Puspita et al. (2020),[55] the oil content (OC) (2) and

encapsulation efficiency (EE) (3)were determined. The test was conducted using a Lambda type 35 Perkin Elmer brand UV-vis spectrometer. In a volumetric flask, 0.1 g of LO microcapsules were crushed and dissolved in 10 mL of *n*-hexane. The solution's absorbance was then measured and quantified using LO's reference calibration curve. The following equations were used to calculate the oil content (OC) and encapsulation efficiency (EE).

$$\text{Oil content } (\%) = \frac{W1 \text{ (g)}}{W2 \text{ (g)}} \times 100\% \tag{2}$$

$$\text{Encapsulation Efficiency } (\%) = \frac{W1 \text{ (g)}}{W \text{ (g)}} \times 100\% \tag{3}$$

where W = weight of microcapsules; W1 = amount of oil coated; and W2 = weight of LO used.

Particle size measurement. A PSA Beckman Coulter LS 13 320 with an optical Fraunhofer and a water carrier was used to measure particle size.

Morphological measurement. A JEOL JSM-6510 SEM tool, a 10 kV electrical detector, and BEI (Backscattered Electron Image) were used to perform morphological measurements.

Infrared fourier transform (FTIR). The FTIR spectra were recorded on a Perkin Elmer spectrum-100 brand at 450–4000 cm^{-1} using a KBr disk.

Thermal stability. A thermogravimetric analyzer (TGA) brand TG 209 F1 Libra, NETZSCH, Germany, with a temperature range of 30–750 °C and a heating rate of 20 °C per minute under a nitrogen atmosphere was used to study thermal stability.

The kinetics of LO release from microcapsules

1 g of LO microcapsules was dissolved in 10 mL of *n*-hexane and then sonicated at a constant frequency and temperature (50 ± 2 °C). 2 mL of aliquot was taken away every 15 minutes for two hours. The aliquot's absorbance was also measured at a 256 nm observation wavelength and quantified using the LO standard curve. The aliquot was added back to the main solution after being quantified.

Referring to the reported procedures, the release mechanism based on kinetic parameters was also investigated based on the Avrami kinetic eqn (4) applied for essential oil release.[18,56–61]

$$\ln(-\ln R) = n \ln(t) + n \ln K(t) \tag{4}$$

Data were used to calculate the release rate constant *k* and the release parameter of *n* from the slope and intercept of the linear regression. A similar procedure was repeated at various temperatures (30–60 °C).

Microcapsule storage stability

The storage stability of the LO microcapsule was tested based on Ja'far *et al.* (2012).[62] A suspension of 0.1 g of LO microcapsules was stored at room temperature for 3 weeks. The amount of volatile oil released in the suspension was observed weekly using a UV-vis spectrophotometer. The OC and EE were then calculated with eqn (2) and (3).

Immobilization of microcapsule on cotton fabric

Immobilization of the LO microcapsules was performed following a method reported by Hunafa *et al.* (2021).[63] A cotton fabric of 10 × 10 cm was dipped into 100 mL of a 20% (v/v) microcapsule suspension, 4% (w/v) citric acid binder, and 1.5% (w/v) sodium phosphate catalyst. The mixture was further stirred for 30 minutes. The dipped sample was then inserted into the padder tool (Werner Mathis AG) at 100% Wet Pick Up (WPU) settings and dried at room temperature. Upon SEM observation, the morphology of the immobilized fabric was further revealed. Afterward, the sample underwent a Launder-O-meter for the washing resistance test up to 1, 2, 3, 4, and 5 times for home washing (SNI ISO 105-C06 test standard: 2010). The equation was used to calculate the increase in fabric weight following treatment (5).

$$\text{Add on } (\%) = \frac{M_a - M_b \text{ (g)}}{M_b \text{ (g)}} \times 100\% \tag{5}$$

where M_a = weight after treatment and M_b = weight before treatment.

Antibacterial activity

The antibacterial activity test was carried out in the same way that it was carried out by Costa *et al.* (2014) using the disc diffusion method.[4] Antibacterial activity testing was not only carried out on a fabric containing LO microcapsules but also against LO and LO microcapsules. Due to the prevalence of skin-associated bacteria, Gram-positive strains of *Staphylococcus aureus* (ATCC 6538) and *Staphylococcus epidermidis* (ATCC 11228), and Gram-negative strains of *Escherichia coli* (ATCC 11229) and *Klebsiella pneumoniae* (ATCC 2357) were chosen for testing. Firstly, microbial strains were cultured overnight at about 10^5 CFU mL^{-1} with sterile saline solution. On an agar medium with MHA for Gram-positive bacteria and NA for Gram-negative bacteria, a 500 μL bacterial suspension was laid out. Empty sterile discs were impregnated with 20 μL LO/ microcapsules/fabric immobilized by LO microcapsules. 100 ppm of amoxicillin and *n*-hexane were employed as positive and negative controls. A zone of inhibition (ZoI/mm) was used to measure antimicrobial activity.

Statistics test

The software Statistical Package for Social Sciences (SPSS) Version 23 was used to conduct the statistical analysis (SPSS Inc., Chicago, USA). Using Duncan's multiple range test and an analysis of variance (ANOVA) at a 95% confidence level ($p \leq 0.05$), it was possible to identify any significant differences between the samples.[64] The mean standard deviation was calculated after a triplicate measurement.

Conclusions

Alginate/gelatin-based microcapsules effectively coacervated LO by using a 15% CaCl$_2$ crosslinker with a yield, EE, and OC of 39.91 ± 3.10%, 78.33 ± 7.53%, and 90.27 ± 5.84%, respectively. Most of the microcapsules have a spherical and agglomerated

shape with an average particle size of 1.394 μm. The LO microcapsules demonstrated the lowest release rate constant with the first-order mechanism. The LO microcapsules showed a good attachment onto the fabric with $22.01 \pm 1.69\%$ mass reduction after 5 cycles of washing. The microcapsules' antibacterial test indicated a moderate inhibition of *S. aureus*, *S. epidermidis*, *E. coli*, and *K. pneumoniae*. However, further investigation must be performed, in particular, to improve the durability of the LO microcapsules immobilized onto the fabric. Thus, the antibacterial LO microcapsules might be applied extensively for cosmetic textiles.

Author contributions

EJ was the main project leader and conceived the overall research idea. LP, EJ, TW, and ASM performed the experiments and data collection. LP, DRE, JA, AH, and EJ were substantially involved in the data analysis. LP and EJ drafted the manuscript and JA finalized it. All authors read and approved the final manuscript before submission.

Conflicts of interest

There are no conflicts to declare.

Acknowledgements

References

1 L. Galovičová, P. Borotová, N. L. Vukovic, M. Vukic, S. Kunová, P. Hanus, P. Ł. Kowalczewski, L. Bakay and M. Kačániová, *Agronomy*, 2022, **12**, 735.

2 M. S. Al-Aamri, N. M. Al-Abousi, S. S. Al-Jabri, T. Alam and S. A. Khan, *J. Taibah Univ. Medical Sci.*, 2018, **13**, 108–112.

3 S. Jafari, S. Esfahani, M. R. Fazeli, H. Jamalifar, M. Samadi, N. Samadi, A. N. Toosi, M. R. S. Ardekani and M. Khanavi, *Int. J. Biol. Chem.*, 2011, **5**, 258–265.

4 R. Costa, C. Bisignano, A. Filocamo, E. Grasso, F. Occhiuto and F. Spadaro, *J. Essent. Oil Res.*, 2014, **26**, 400–408.

5 R. S. Lemes, C. C. F. Alves, E. B. B. Estevam, M. B. Santiago, C. H. G. Martins, T. C. L. Dos Santos, A. E. M. Crotti and M. L. D. Miranda, *An. Acad. Bras. Cienc.*, 2018, **90**, 1285–1292.

6 N. Torimiro, B. R. Adegun, O. E. Abioye and R. K. Omole, *Adv. Microbiol.*, 2020, **10**, 214–223.

7 W. R. Glomm, P. P. Molesworth, E. M. Sandru, L. T. Truong, A. Brunsvik and H. Johnsen, *Appl. Sci.*, 2021, **11**, 3956.

8 E. Julaeha, R. Nugeraha, M. Nurzaman, D. Kurnia, T. Wahyudi and Y. Rosandi, *J. Phys.: Conf. Ser.*, 2018, **1080**, 012038.

9 R. Tekin, N. Bac and H. Erdogmus, *Macromol. Symp.*, 2013, **333**, 35–40.

10 X. Jun-xia, Y. Hai-yan and Y. Jian, *Food Chem.*, 2011, **125**, 1267–1272.

11 A. Martin, S. Varona, A. Navarrete and M. J. Cocero, *Open Chem. Eng. J.*, 2010, **4**, 31–41.

12 Y. P. Timilsena, M. A. Haque and B. Adhikari, *Food Nutr. Sci.*, 2020, **11**, 481–508.

13 F. H. Yusop, S. F. A. Manaf and F. Hamzah, *Chem. Eng. Res. Bull.*, 2017, **19**, 50.

14 M. Saravanan and K. P. Rao, *Carbohydr. Polym.*, 2010, **80**, 808–816.

15 N. Devi and D. K. Kakati, *J. Food Eng.*, 2013, **117**, 193–204.

16 E. F. De Matos, B. S. Scopel and A. Dettmer, *J. Environ. Chem. Eng.*, 2018, **6**, 1989–1994.

17 E. Julaeha, M. Nurzaman, D. R. Eddy, D. Kurnia, S. Puspita, Y. Rosandi, T. Wahyudi and J. Al Anshori, *Rev. Chim.*, 2020, **71**, 146–155.

18 E. Julaeha, P. Puspita, D. E. Rakhmawaty, T. Wahyudi, M. Nurzaman, J. Nugraha, T. Herlina and J. Al Anshori, *RSC Adv.*, 2021, **11**, 1743–1749.

19 E. Julaeha, D. R. Eddy, T. Wahyudi, B. A. Ningsih, M. Nurzaman, N. Permadi, T. Herlina and J. Al Anshori, *ChemistrySelect*, 2022, **7**, 1–7.

20 S. Tie, X. Zhang, H. Wang, Y. Song and M. Tan, *J. Agric. Food Chem.*, 2020, **68**, 3163–3170.

21 L. P. H. Bastos, J. Vicente, C. H. C. dos S. Santos, M. G. de Carvalho and E. E. Garcia-Rojas, *Food Hydrocolloids*, 2020, **102**, 105605.

22 J. Jayanudin and H. Heriyanto, *WCEJ*, 2021, **5**(2), 37–43.

23 S. Rojas-Moreno, G. Osorio-Revilla, T. Gallardo-Velázquez, F. Cárdenas-Bailón and G. Meza-Márquez, *J. Microencapsulation*, 2018, **35**, 165–180.

24 Z. Xiao, W. Liu, G. Zhu, R. Zhou and Y. Niu, *Flavour Fragrance J.*, 2014, **29**, 166–172.

25 S. Karagonlu, G. Başal, F. Ozyıldız and A. Uzel, *Int. J. Eng. Res. Technol.*, 2018, **4**, 263122.

26 F. Abasalizadeh, S. V. Moghaddam, E. Alizadeh, E. Akbari, E. Kashani, S. M. B. Fazljou, M. Torbati and A. Akbarzadeh, *J. Biol. Eng.*, 2020, **14**, 1–22.

27 N. E. Simpson, C. L. Stabler, C. P. Simpson, A. Sambanis and I. Constantinidis, *Biomaterials*, 2004, **25**, 2603–2610.

28 D. Massella, S. Giraud, J. Guan, A. Ferri and F. Salaün, *Environ. Chem. Lett.*, 2019, **17**, 1787–1800.

29 H. Upadhayay, S. Jahan and M. Upreti, *IOSR J. Polym. Text. Eng.*, 2016, **3**, 8–14.

30 A. M. Falcatan, G. S. Fernandez, A. M. Falcatan, L. M. Labaclado and A. I. Atienza, *J. Text. Sci. Fash. Technol.*, 2020, **6**, 4–8.

31 W. Y. Wang, J. C. Chiou, J. Yip, K. F. Yung and C. W. Kan, *Coatings*, 2020, **10**, 1–13.

32 Q. B. Xu, X. T. Ke, L. W. Shen, N. Q. Ge, Y. Y. Zhang, F. Y. Fu and X. D. Liu, *Int. J. Biol. Macromol.*, 2018, **111**, 796–803.

33 T. K. Varkey, S. Baby and J. Mathew, *Asian J. Chem.*, 2013, **25**, 7871–7875.

34 D. Sharma and H. Vashist, *J. Plant Sci.*, 2015, **10**, 75–78.

35 I. K. Shakir and S. J. Salih, *Iraqi J. Chem. Pet. Eng.*, 2015, **16**, 11–22.

36 A. J. Wibaldus, P. Ardiningsih and J. Kim, *Khatulistiwa*, 2016, **5**, 44–51.

37 T. Wahyudi, A. S. Mulyawan, C. Kasipah, U. Prayudie and E. Julaeha, *Arena Tekst.*, 2017, **32**(1), 1–8.

38 H. Bora, M. Kamle, D. K. Mahato, P. Tiwari and P. Kumar, *Plants*, 2020, **9**, 1–25.

39 L. Lin, C. Chuang, H. Chen and K.-M. Yang, *Foods*, 2019, **8**, 1–11.

40 K. A. Selim, S. S. Alharthi, A. M. Abu El-Hassan, N. A. Elneairy, L. A. Rabee and A. G. Abdel-Razek, *Molecules*, 2021, **26**, 6109.

41 H. Kaur, P. Pancham, R. Kaur, S. Agarwal and M. Singh, *J. Biomater. Nanobiotechnol.*, 2020, **11**, 215–236.

42 J. M. Souza, A. L. Caldas, S. D. Tohidi, J. Molina, A. P. Souto, R. Fangueiro and A. Zille, *Rev. Bras. Farmacogn.*, 2014, **24**, 691–698.

43 R. Stojanovic, A. Belscak-Cvitanovic, V. Manojlovic, D. Komes, V. Nedovic and B. Bugarski, *J. Sci. Food Agric.*, 2012, **92**, 685–696.

44 J. Ghosh, G. Vishwakarma, S. Das and T. Pradeep, *J. Phys. Chem. C*, 2021, **125**, 4532–4539.

45 J. Lelito, *Materials*, 2020, **13**, 1–9.

46 A. Sarkar, S. Sanyal, T. K. Bandyopadhyay and S. Mandal, *Mater. Sci. Technol.*, 2019, **35**, 2054–2068.

47 S. Majoni and J. M. Hossenlopp, *Adv. Phys. Chem.*, 2014, **12**, 710487.

48 A. Sharkawy, I. P. Fernandes, M. F. Barreiro, A. E. Rodrigues and T. Shoeib, *Ind. Eng. Chem. Res.*, 2017, **56**, 5516–5526.

49 C. D. Ferreira, E. J. L. da Conceição, B. A. S. Machado, V. S. Hermes, A. de Oliveira Rios, J. I. Druzian and I. L. Nunes, *Food Bioprocess Technol.*, 2016, **9**, 124–136.

50 N. A. Ibrahim, B. M. Eid, N. A. Abd El-Ghany and E. M. Mabrouk, *J. Text. Inst.*, 2020, **111**, 381–393.

51 P. Monllor, L. Capablanca, J. Gisbert, P. Díaz, I. Montava and Á. Bonet, *Text. Res. J.*, 2010, **80**, 631–635.

52 Z.-H. Li, M. Cai, L. Yuan-Shuai, P.-L. Sun and L. Shao-Lei, *Molecules*, 2019, **24**, 1–10.

53 J. S. F. de Araújo, E. L. de Souza, J. R. Oliveira, A. C. A. Gomes, L. R. V. Kotzebue, D. L. da Silva Agostini, D. L. V. de Oliveira, S. E. Mazzetto, A. L. da Silva and M. T. Cavalcanti, *Int. J. Biol. Macromol.*, 2020, **143**, 991–999.

54 M. A. Ferhat, M. N. Boukhatem, M. Hazzit, B. Y. Meklati and F. Chemat, *Electron. J. Biotechnol.*, 2016, **1**, 30–41.

55 S. Puspita, D. R. Eddy, T. Wahyudi and E. Julaeha, *J. Kim. Valensi*, 2020, **6**(1), 104–110.

56 S. Phunpee, U. R. Ruktanonchai, H. Yoshii, S. Assabumrungrat and A. Soottitantawat, *Biosci., Biotechnol., Biochem.*, 2017, **81**, 718–723.

57 Y. Yang, X. Li and S. Zhang, *RSC Adv.*, 2018, **8**, 29980–29987.

58 J. D. W. Rodríguez, S. Peyron, P. Rigou and P. Chalier, *PLoS One*, 2018, **13**, e0207401.

59 A. Sultana and H. Yoshii, *Biosci., Biotechnol., Biochem.*, 2019, **83**, 738–746.

60 K. Khounvilay, B. N. Estevinho and W. Sittikijyothin, *Eng. J.*, 2019, **23**, 217–227.

61 T. Cui, C. Chen, A. Jia, D. Li, Y. Shi, M. Zhang, X. Bai, X. Liu and C. Liu, *J. Funct. Foods*, 2021, **83**, 104542.

62 F. Jaâfar, M. A. Lassoued, M. Sahnoun, S. Sfar and M. Cheikhrouhou, *Fibers Polym.*, 2012, **13**, 346–351.

63 C. A. Hunafa, D. D. Nabila, D. N. I. Sari, R. Nurkhotimah, M. A. Lestari, T. Wahyudi and E. Julaeha, *Arena Tekst.*, 2021, **36**(2), 83–90.

64 J. K. Mohammed, A. A. Mahdi, C. Ma, A. E. Elkhedir, Q. A. Al-Maqtari, W. Al-Ansi, A. Mahmud and H. Wang, *J. Food Meas. Charact.*, 2021, **15**, 155–169.